contain intact M'(NS) rings (see below).

Origins of Specific Target-Transmetalator Interactions. We now offer an explanation for our conclusion that $(\mu_4\text{-O})(N,py)_4Cu_2(Ni(H_2O))_2Cl_6$ are the stickiest members of the $(\mu_4\text{-O})(N,py)_4Cu_{4-x}(Ni(H_2O))_xCl_6$ target family.

Table VI summarizes the rate laws for transmetalation of this family with sticky transmetalator B_3. Table VII gives the number of each kind of edge and face in $(\mu_4\text{-O})N_4Cu_{4-x}(Ni(H_2O))_xCl_6$ complexes. The structural features that predominate through maxima with increasing x are (a) Cu-Cl-Ni edges at $x = 2$, (b) Cu_2Ni faces at $x = 1$, and (c) $CuNi_2$ faces at $x = 3$.

Table VII indicates that the greatest number (6) of Cu-Cl-Ni edges and $CuNi_2$ faces is found in $(\mu_4\text{-O})(N,py)_4Cu_{4-x}(Ni(H_2O))_xCl_6$ targets at $x = 2$ and $x = 3$.[22] Saturated kinetic behavior (rate law 4 or 6) is observed at these same values of x. The indication is that Cu-Cl-Ni edges and $CuNi_2$ faces both contribute to precursor stability, with the edges playing the dominant role. However, we cannot strongly favor one factor over the other, since small temperature variations can cause transmetalation rate law changes from eq 6 to eq 4 (see, for example, Figures 3 and 4 of ref 9).

(22) $(N,py)Cu_3NiX$ complexes contain no $CuNi_2$ faces (Table VII).

Conclusions. The rate laws for monotransmetalation of $(\mu_4\text{-O})(N,py)_4Cu_{4-x}(Co,Ni(H_2O))_xX_6$ targets with $M'(NS)_n$ transmetalators B_1-B_3 and E are a sensitive function of x and M' because Co-X and Ni-X bonds are weaker than Cu-X bonds in these targets and $M'(NS)_n$ have different affinities for a fixed target. Precursor formation leads to specific association of M' in $M'(NS)_n$ with a copper(II) center of the target. This association helps to direct specific replacement of copper(II) with M'.

Acknowledgment. This work was supported by Biomedical Research Support Grant RR07143 from the Department of Health and Human Services and Grants INT-8715384 and CHE8717556 from the National Science Foundation, which are gratefully acknowledged. S.A.-S. thanks the Saudi Arabian Government for a graduate fellowship, and M.A.E.-S. and A.E.-T. thank Alexandria University, Alexandria, Egypt, for study leave to collaborate on this project.

Supplementary Material Available: Table III, containing kinetic data for monotransmetalation of D (6 pages). Ordering information is given on any current masthead page.

Contribution from the Department of Chemistry,
University of Wisconsin—Madison, Madison, Wisconsin 53706

Thermal Isomerization of Regiospecifically ^{10}B-Labeled Icosahedral Carboranes

Gary M. Edvenson and Donald F. Gaines*

Received September 1, 1989

Thermal treatment of regiospecifically ^{10}B-enriched (96%) 3-(^{10}B)-1,2-$C_2{}^nB_9H_{12}$ and 2-(^{10}B)-1,7-$C_2{}^nB_9H_{12}$ (^nB = boron with normal isotopic abundances) followed by ^{10}B and ^{11}B NMR analysis reveal that (1) 3-(^{10}B)-1,2-$C_2{}^nB_9H_{12}$ undergoes rearrangements that completely scramble the enriched boron atom, (2) these rearrangements occur at a rate faster than the conversion of 1,2-$C_2B_{10}H_{12}$ to 1,7-$C_2B_{10}H_{12}$, (3) the 1,7-$C_2B_{10}H_{12}$ that is formed does not re-form 1,2-$C_2B_{10}H_{12}$ at a detectable rate, and (4) at temperatures at which 1,2-$C_2B_{10}H_{12}$ forms 1,7-$C_2B_{10}H_{12}$ at a significant rate, the latter undergoes no further rearrangements. The movement of ^{10}B at 350 °C in 1,2-$C_2B_{10}H_{12}$ is compared to the movement predicted by various isomerization mechanisms. The mechanism that appears to give the closest agreement involves a 12-vertex nido intermediate. It was found that a number of previously considered mechanisms, including simple exchange between two boron sites, triangular face rotation in an icosahedron, diamond-square-diamond twist, and rotation of pentagonal pyramids, are extensions of the nido intermediate mechanism. The synthesis and thermal rearrangement of 3-F-3-(^{10}B)-1,2-$C_2{}^nB_9H_{11}$ demonstrate that independent intramolecular fluorine migration does not occur during rearrangement.

Introduction

o-Carborane,[1] 1,2-$C_2B_{10}H_{12}$, was first prepared from the reaction of decaborane with acetylene in Lewis basic solvents.[2] This icosahedral molecule with adjacent carbons was found to undergo an irreversible thermal rearrangement at 450 °C to produce a meta isomer,[3] 1,7-$C_2B_{10}H_{12}$, in which the carbons are no longer adjacent. At 620 °C the meta isomer rearranges reversibly to the para isomer, 1,12-$C_2B_{10}H_{12}$ (Figure 1).[4,5] The chemistry of the carboranes and their applications in the synthesis of high-temperature polymers has been reviewed.[6]

Postulates regarding isomerization mechanisms followed closely on the heels of the thermal rearrangement studies. The principal mechanistic proposals are shown in Figure 2. The conversion of *o*- to *m*-carborane, for example, may be viewed as an intramolecular rearrangement based on a cuboctahedral intermediate[7] (Figure 2a), a rotation of the two fused pentagonal-pyramid cluster halves[2] (Figure 2b), a triangular face rotation in an icosahedron (Figure 2c), a diamond-square-diamond twist (Figure 2d), or a 12-vertex nido intermediate (Figure 2e).

The use of boron-halogenated carborane derivatives provided an additional external cluster atom label and allowed somewhat more detailed analysis of possible rearrangement pathways. The product distribution from the thermal isomerization of 9-bromo-*o*-carborane, for example, appeared to be consistent with a variation of the cuboctahedral intermediate mechanism in which selected triangular faces rotated in the transition state.[8] The products from the thermal isomerization of 9-chloro-*m*-carborane were also consistent with the cuboctahedral intermediate mechanism, but in this case a different set of triangular faces was required to rotate.[9] Rotation of pentagonal pyramids (Figure 2b) and rotation of a triangular face in the ground icosahedral state[10] (Figure 2c) were considered unlikely mechanisms at the

(1) the following nomenclature is used in this paper: carborane = dicarba-*closo*-dodecaborane(**12**); *o*-carborane, *m*-carborane, and *p*-carborane = 1,2-, 1,7-, and 1,12-dicarba-*closo*-dodecaborane(12), respectively; ^nB = boron atoms with normal isotopic abundances (80% ^{11}B, 20% ^{10}B).
(2) (a) Fein, M.; Bobinski, J.; Mayes, N.; Schwartz, N.; Cohen, M. S. *Inorg. Chem.* **1963**, *2*, 1111-1115. (b) Heying, T. L.; Ager, J. W., Jr.; Clark, S. L.; Mangold, D. J.; Goldstein, H. L.; Hillman, M.; Polak, R. J.; Szymanski, J. W. *Ibid.* **1963**, *2*, 1089-1092.
(3) Grafstein, D.; Dvorak, J. *Inorg. Chem.* **1963**, *2*, 1128-1133.
(4) Papetti, S.; Heying, T. L. *J. Am. Chem. Soc.* **1964**, *86*, 2295.
(5) Stanko, V. I.; Brattsev, V. A.; Gol'tyapin, Yu. V. *Zh. Obshch. Khim.* **1969**, *39*, 2686-2688.
(6) Grimes, R. N. *Carboranes*; Academic Press: New York, 1970.
(7) Hoffmann, R.; Lipscomb, W. N. *Inorg. Chem.* **1963**, *1*, 231-232.
(8) Kaesz, H. D.; Bau, R.; Beall, H. A.; Lipscomb, W. N. *J. Am. Chem. Soc.* **1967**, *89*, 4218-4220.
(9) Hart, H. V.; Lipscomb, W. N. *J. Am. Chem. Soc.* **1969**, *91*, 771-772.
(10) Muetterties, E. L.; Knoth, W. N. *Polyhedral boranes*; Marcel Dekker: New York, 1968; p 70.

0020-1669/90/1329-1210$02.50/0

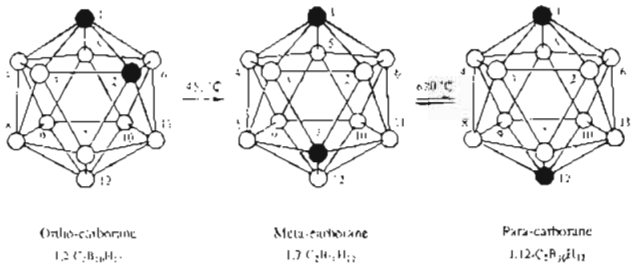

Figure 1. Structures, numbering system, and observed thermal rearrangements of the icosahedral $C_2B_{10}H_{12}$ carboranes.

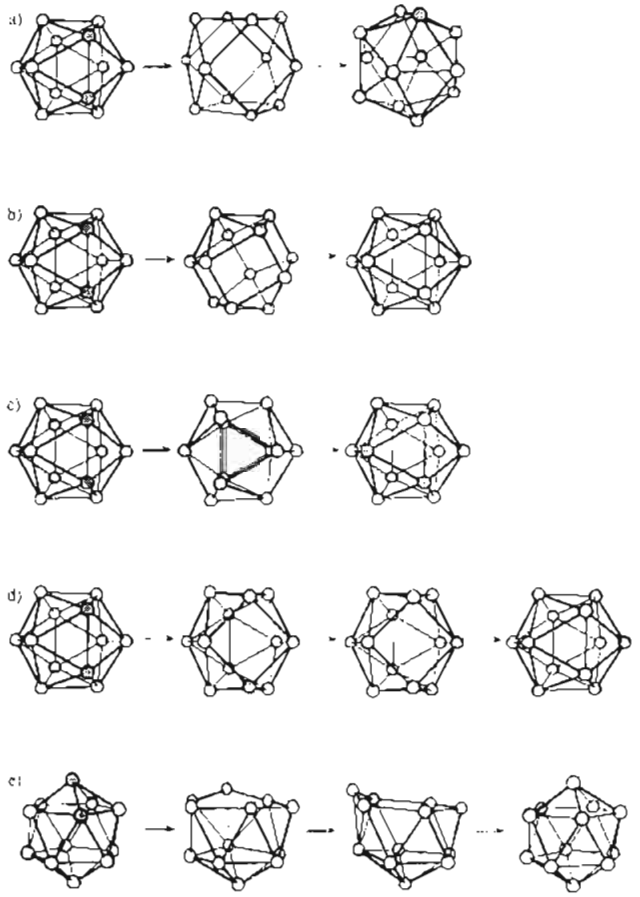

Figure 2. Several postulated mechanisms for thermal rearrangements of icosahedral carboranes.

time. The original cuboctahedral intermediate mechanism (Figure 2a) successfully modeled the formation of 5,12-Cl_2-*m*-$B_{10}H_8C_2Me_2$ from 9,12-Cl_2-*o*-$B_{10}H_8C_2Me_2$[11] whereas triangular face rotations in a cuboctahedral intermediate were required to model the initial distribution of ortho isomers produced from the same starting material.

Finally, the rotation of pentagonal pyramids accounted best for the thermal rearrangement products of the chlorophosphacarboranes, 12-Cl-1,2-$CHPB_{10}H_9$, 1,7-$CHPB_{10}H_9Cl$, and 1,12-$CHPB_{10}H_9Cl$.[12] The diamond–square–diamond twist mechanism, which involves opening a diamond in the icosahedron to a square and rotating it (Figure 2d), was considered and rejected as a mechanistic model for the chlorophosphacarborane rearrangements as it failed to predict the observed products. A significantly different mechanistic postulate introduced in this study involved the opening of the closo icosahedral structure to a nido structure. Diamond–square–diamond rearrangements on the edge of the nido intermediate produce different configurations that may reclose to a new icosahedral isomer (Figure 2e). Discrepancies between the observed product distributions and those predicted on the basis of random C and P locations in the intermediate nido structure discouraged the authors from favoring this mechanism.[12]

At temperatures at which ortho to ortho and ortho to meta isomerizations are observed in the *B*-halocarboranes, the *B*-halo-*m*-carboranes formed do not continue to isomerize.[8,11,12] Rearrangements in *B*-halo-*m*-carboranes have been observed only at temperatures that also produce para isomers.[9,12] None of the mechanistic proposals to date have been able to account for the higher barrier to rearrangement in *m*-carboranes relative to *o*-carboranes.

Recently, Wu and Jones[13] have studied the thermal rearrangement of a bridged *o*-carborane derivative in which an exopolyhedral three atom chain connects a cage carbon to one of its adjacent borons. They suggest an extended triangle rotation, ETR, mechanism to rationalize their pyrolysis data and data in the literature. The ETR mechanism is a more detailed extension of the rotation of icosahedral triangular faces (Figure 2c).

With the exception of the original 1,2-$C_2B_{10}H_{12}$ to 1,7-$C_2B_{10}H_{12}$ and 1,12-$C_2B_{10}H_{12}$ conversions and the study just cited,[13] all of the mechanistic studies to date have been based on experimental investigations of halogenated carboranes. While carborane frameworks labeled in this way provide a means of detecting boron atom rearrangements, the identification of the multitude of isomers produced became a formidable limiting factor in some studies.[11,12] The intermolecular exchange of halogen substituents between carborane frameworks was ruled out in the studies described above, but intermolecular exchange of iodine in similar systems has been observed.[14] Intramolecular migration of halogen substituents during icosahedral rearrangements was not investigated.

The icosahedral $C_2B_{10}H_{12}$ carboranes are easily reduced to $C_2B_{10}H_{12}^{2-}$ dianions,[3,15] which form 13-vertex *closo*-metallacarborane complexes such as (π-C_5H_5)Co($C_2B_{10}H_{12}$).[16] The 12-vertex *nido*-$C_2B_{10}H_{12}$ structure that has been postulated as an isomerization intermediate (Figure 2e) is structurally similar to the 13-vertex metallacarborane minus the metal atom and as a neutral species is two electrons short of being a stable nido structure. The discrete thermal opening of an icosahedron is suggested by the formation of (π-C_5H_5)$CoC_2B_9H_{11}$ from the gas-phase reaction of 1,2-$C_2B_{10}H_{12}$ and (π-C_5H_5)$Co(CO)_2$ at 300 °C.[17] The 2-fold diamond–square–diamond rearrangement within the nido intermediate in Figure 2e is similar to the mechanism used to explain the rapid interconversion of (π-C_5H_5)Co(7,9-$C_2B_{10}H_{12}$) and (π-C_5H_5)Co(7,11-$C_2B_{10}H_{12}$)[16] but without the metal vertex. A mechanism similar to that shown in Figure 2e was proposed to account for the fluxional rearrangement of the quasi-icosahedral $(CH_3)_4C_4B_8H_8^{2-}$ ion and the formation of various ferracarboranes from reactions involving this ion.[18] On the basis of such chemical precedent and molecular orbital symmetry considerations, the authors of a review of carborane rearrangements[19] favor the nido intermediate mechanism to explain the thermal rearrangement of icosahedral carboranes. In addition, several theoretical studies of borane and carborane cluster rearrangements have appeared recently.[20]

We have undertaken an investigation of icosahedral carborane rearrangements using an isotopic label rather than a substituent

(11) Hart, H. V.; Lipscomb, W. N. *Inorg. Chem.* **1973**, *12*, 2644–2649.
(12) Wong, H. S.; Lipscomb, W. N. *Inorg. Chem.* **1975**, *14*, 1350–1357.
(13) Wu, S.-h.; Jones, M., Jr. *J. Am. Chem. Soc.* **1989**, *111*, 5373–5384.
(14) Zakharkin, L. I.; Kalinin, V. N. *Izv. Akad. Nauk SSSR, Ser. Khim.* **1969**, 607–611.
(15) (a) Zakharkin, L.; Kalinin, V.; Podvisotskaya, L. *Izv. Akad. Nauk SSSR, Ser. Khim.* **1967**, 2310–2316. (b) Zakharkin, L.; Kalinin, V.; *Ibid.* **1969**, 194. (c) Stanko, V.; Gol'tyapin, Yu. V.; Brattsev, V. *Zh. Obshch. Khim.* **1969**, *39*, 1175.
(16) Dustin, D. F.; Dunks, G. B.; Hawthorne, M. F. *J. Am. Chem. Soc.* **1973**, *95*, 1109–1115.
(17) Miller, V. R.; Sneddon, L. G.; Beer, D. C.; Grimes, R. N. *J. Am. Chem. Soc.* **1974**, *96*, 3090–3098.
(18) Grimes, R. N.; Pipal, J. R.; Sinn, E. *J. Am. Chem. Soc.* **1979**, *101*, 4172–4180.
(19) Stanko, V. I.; Brattsev, V. A.; Knyazev, S. P. *Usp. Khim.* **1979**, *48*, 241–279.
(20) (a) Wales, D. J.; Stone, A. J. *Inorg. Chem.* **1987**, *26*, 3845–3850. (b) Wales, D. J.; Mingos, D. M. P.; Zhenyang, L. *Inorg. Chem.* **1989**, *28*, 2754–2764.

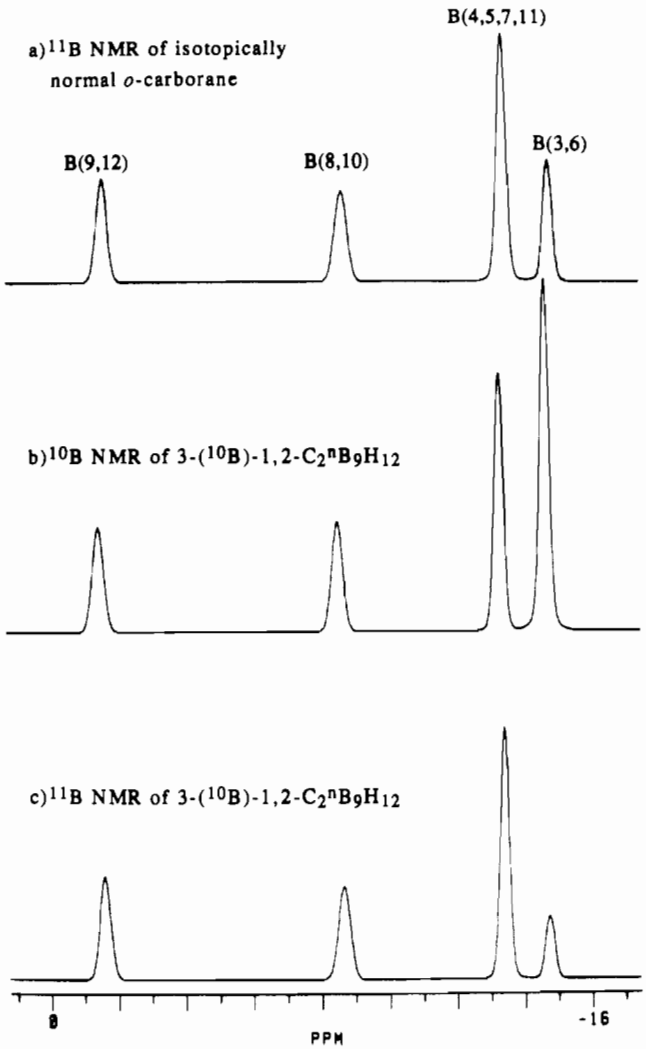

Figure 3. (a) 160.46-MHz ^{11}B NMR spectrum of isotopically normal *o*-carborane. (b) 53.73-MHz ^{10}B NMR spectrum of 3-(^{10}B)-1,2-$C_2{}^nB_9H_{12}$. (c) 160.46-MHz ^{11}B NMR spectrum of 3-(^{10}B)-1,2-$C_2{}^nB_9H_{12}$. All spectra are ^{1}H decoupled.

or heteroatom label. The natural isotopic composition of boron is approximately 81% ^{11}B and 19% ^{10}B,[21] and both isotopes are readily observable by NMR spectroscopy ($I_{^{11}B} = {}^3/_2$; $I_{^{10}B} = 3$). Several boron compounds enriched to 96% ^{10}B are commercially available. We report herein the syntheses of regiospecific ^{10}B isotopically labeled 3-(^{10}B)-1,2-$C_2{}^nB_9H_{12}$, 2-(^{10}B)-1,7-$C_2{}^nB_9H_{12}$, and 3-F-3-(^{10}B)-1,2-$C_2{}^nB_9H_{12}$, investigations of thermally induced rearrangements of the ^{10}B label, and analyses of various postulated rearrangement mechanisms in light of the experimental results.

Results and Discussion

Preparation of 3-(^{10}B)-*o*-Carborane. Regiospecifically ^{10}B-labeled *o*-carborane was prepared by a modification of Hawthorne's boron insertion reaction[22] using 96.2% ^{10}B-enriched $HBCl_2$[23] (eq 1; ^nB = boron with normal isotopic abundances).

$$H^{10}BCl_2 + Na_2[o\text{-}C_2{}^nB_9H_{11}] \xrightarrow{THF} 2NaCl + 3\text{-}(^{10}B)\text{-}1,2\text{-}C_2{}^nB_9H_{12} \quad (1)$$

Figure 3 shows an ^{11}B NMR spectrum of isotopically normal *o*-carborane along with the ^{10}B and ^{11}B NMR spectra of 3-(^{10}B)-1,2-$C_2{}^nB_9H_{12}$. The enrichment and depletion in the B(3,6) resonance of 3-(^{10}B)-*o*-carborane is clearly visible. Integration of the ^{10}B NMR spectrum was normalized on the basis of an isotopic composition for our ^{10}B source of 96.2% ^{10}B. This led to a value of 20.2% ^{10}B in the unenriched positions, which is in close agreement with the expected value of 19.8% and indicates that the insertion was indeed regiospecific.

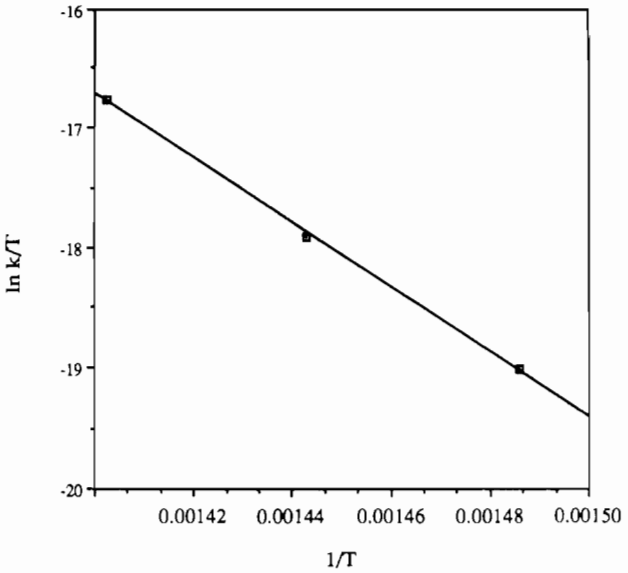

Figure 4. Plot of (ln k)/T vs $1/T$ for the isomerization of *o*- to *m*-carborane at 400, 420, and 440 °C from which activation parameters for the isomerization were calculated.

Preparation of 2-(^{10}B)-*m*-Carborane. Regiospecifically ^{10}B-labeled *m*-carborane was prepared by the reaction of 96% ^{10}B-enriched $HBCl_2$ with the lithium salt of the *m*-dicarbollide ion (eq 2).[24] Integration of the ^{10}B NMR spectrum of the *m*-carborane product showed that the insertion was entirely regiospecific.

$$H^{10}BCl_2 + Li_2[m\text{-}C_2{}^nB_9H_{11}] \xrightarrow{Et_2O} 2LiCl + 2\text{-}(^{10}B)\text{-}1,7\text{-}C_2{}^nB_9H_{12} \quad (2)$$

Thermolysis of 3-(^{10}B)-*o*-Carborane. Samples of 3-(^{10}B)-*o*-carborane were sealed under vacuum in glass ampules and heated in a tube furnace (see Experimental Section) at temperatures ranging from 350 to 480 °C. *o*- and *m*-Carborane from these samples were separated by thin-layer rotary chromatography and analyzed by ^{11}B and ^{10}B NMR spectroscopy. The degree of scrambling of the labeled boron atom within *o*-carborane and the amount of *m*-carborane formed increased with time and temperature. After 144 h at 350 °C only 5% of the *o*-carborane was converted to *m*-carborane and the B(3,6) and B(4,5,7,11) positions in *o*-carborane were still heavily enriched, whereas, after 6 h at 450 °C, 85% of the *o*-carborane was isomerized to *m*-carborane and the label in the *o*-carborane that remained was entirely scrambled. Complete conversion of *o*- to *m*-carborane and a trace of *p*-carborane occurred after 24 h at 480 °C. Samples heated for intermediate times and temperatures showed that the ^{10}B label moved first to the B(4,5,7,11) position followed by the B(8,10) position and finally the B(9,12) position.

Identical mass spectroscopic analyses for isomerized and unisomerized samples indicate that the rearrangement we are observing is not the result of intermolecular exchange of boron atoms. Isomerization of *o*-carborane via a *m*-carborane intermediate was tested by heating a sample of pure *m*-carborane at 370 °C for 96 h. No *o*-carborane could be detected in the ^{11}B NMR spectrum of this sample in which we could have detected 1 part in 5000. Thus, we conclude that the observed isomerization is a result of intramolecular ortho to ortho rearrangements.

Rate Determinations. Samples of isotopically normal *o*-carborane were heated at 400, 420, and 440 °C. The rate of isomerization of *o*-carborane to *m*-carborane for these samples

(21) Shima, M. *Geochim. Cosmochim. Acta* **1963**, *27*, 911–913.
(22) Hawthorne, M. F.; Wegner, P. A. *J. Am. Chem. Soc.* **1968**, *90*, 896–901.
(23) Zweifel, G. *J. Organomet. Chem.* **1967**, *9*, 215–221.
(24) Roscoe, J. S.; Kongpricha, S.; Papetti, S. *Inorg. Chem.* **1970**, *9*, 1561–1563.

was determined from the relative integrals of the ^{11}B NMR resonances of *o*- and *m*-carborane. The rate of isomerization was $(3.73 \pm 0.15) \times 10^{-6}$ s^{-1}, $(1.15 \pm 0.05) \times 10^{-5}$ s^{-1}, and $(3.74 \pm 0.15) \times 10^{-5}$ s^{-1} at 400, 420, and 440 °C, respectively. Activation parameters for the isomerization are $\Delta G^{\ddagger} = 57.3 \pm 0.4$ kcal mol^{-1}, $\Delta H^{\ddagger} = 54 \pm 15$ kcal mol^{-1}, and $\Delta S^{\ddagger} = -5 \pm 11$ cal mol^{-1} K^{-1}, which are in close agreement with earlier studies.[25] Figure 4 shows a graph of $(\ln k)/T$ vs $1/T$ for the *o*- to *m*-carborane isomerization from which the activation parameters were calculated. Extrapolation of these data to 350 °C gives a rate of conversion of *o*- to *m*-carborane of 1.03×10^{-7} s^{-1} at this temperature. An estimate of 9.16×10^{-7} s^{-1} was obtained for the rate of ^{10}B movement within *o*-carborane at 350 °C by observing the initial loss of ^{10}B from the B(3,6) resonance. Since the apparent rate of ^{10}B movement decreases with time as equilibration occurs between labeled boron atoms in different positions, the initially observed rate of ^{10}B movement is probably a lower limit for the rate of the isomerization that gives rise to it. Thus, at 350 °C the rate of *o*-carborane to *o*-carborane isomerization is at least nine times the rate of *o*- to *m*-carborane isomerization.

Thermolysis of 2-(^{10}B)-*m*-Carborane. *m*-Carborane isolated from the thermolysis of 3-(^{10}B)-*o*-carborane for 24 h at 480 °C exhibited a statistically scrambled ^{10}B isotopic distribution, whereas the thermolysis of 3-(^{10}B)-*o*-carborane at 370 °C for 78 h yielded a small amount of *m*-carborane that was heavily enriched with ^{10}B in the B(2,3) and B(4,6,8,11) positions. These isotopic distributions resulted at least in part from isomerizations within *o*-carborane prior to conversion to *m*-carborane, but we could not rule out the possibility of rearrangements occurring within *m*-carborane. Therefore, we carried out an independent thermolysis of a sample of regiospecifically labeled 2-(^{10}B)-*m*-carborane for $5^1/_2$ h at 450 °C (conditions that converted most of a sample of *o*-carborane to *m*-carborane) and found no isomerization detectable by ^{10}B NMR spectroscopy. Another sample heated for 24 h at 470 °C (a temperature just below the 480 °C found earlier to give traces of *p*-carborane) also showed no rearrangement of the ^{10}B label or formation of *o*-carborane. This higher barrier to rearrangement of the *m*-carborane framework relative to *o*-carborane is consistent with the halocarborane studies.[8,10]

Thermolysis of 3-Fluoro-(^{10}B)-*o*-carborane. Previous reports of the thermal rearrangement of 3-fluoro-*o*-carborane indicated that several fluorocarborane isomers are formed[9,24] with 2-fluoro-*m*-carborane as the major rearrangement product after 18 h at 395 °C.[24] To test for intramolecular halogen migration in thermal rearrangements of halocarboranes, we heated a sample of 3-fluoro-3-(^{10}B)-1,2-$C_2{}^nB_9H_{11}$ at 360 °C for 6 days. Intramolecular fluorine migration during rearrangement, if it occurs, would be detected as a change in the ratio of boron in fluorinated and unfluorinated positions in going from starting material to rearranged product. The ^{10}B NMR spectrum of 2-fluoro-*m*-carborane isolated from the above thermolysis showed 97% ^{10}B in the B(2)–F position compared to 96% ^{10}B in the B–F resonance of the 3-fluoro-*o*-carborane starting material. The ^{11}B NMR spectrum of the same 2-fluoro-*m*-carborane sample showed 3.6% ^{11}B in the B(2)–F position compared to 3.8% ^{11}B in the fluorinated position of the enriched starting material. Thus, no fluorine migration has occurred. Interestingly, when a relaxation delay of twice the acquisition time was used, the fluorinated B(2) resonance in 2-fluoro-*m*-carborane gave erroneously low integrals in the ^{10}B NMR spectrum. A relaxation delay of 2 s between pulses brought the ^{10}B integrals into agreement with the complementary ^{11}B integrals. The apparent saturation in the B(2) resonance of 2-fluoro-2-(^{10}B)-*m*-carborane may be the result of coupling between ^{10}B and ^{19}F. A well-resolved, 16-Hz ^{10}B–^{19}F coupling constant was measured for the B(2) resonance of 2-fluoro-2-(^{10}B)-*m*-carborane in contrast to the broad singlet observed for the B(3) resonance of 3-fluoro-3-(^{10}B)-*o*-carborane.

Thermolysis of 3-(^{10}B)-*o*-Carborane at 350 °C. Figure 5a shows the spectral distribution of ^{10}B in *o*-carborane samples that were heated at 350 °C for times ranging from 1 to 38 days. Error bars on the *y* axis represent a 3% integration error that was determined by the reproducibility of integrations on samples of known isotopic composition. (See Experimental Section for details of data processing.)

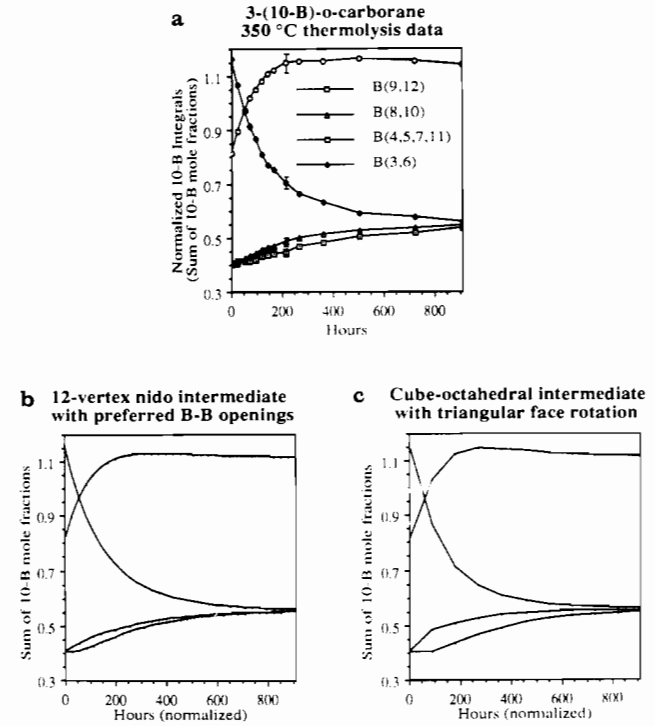

Figure 5. Observed distribution of ^{10}B in *o*-carborane with time as a result of isomerization of 3-(^{10}B)-1,2-$C_2{}^nB_9H_{12}$ at 350 °C and representative simulated ^{10}B distributions based on the criteria indicated in the label of each graph. Error bars on the *y* axis represent a 3% integration error that was determined by the reproducibility of integrations on samples of known isotopic composition.

Parts b and c of Figure 5 show comparisons between the 350 °C thermolysis data and three selected mechanisms. These plots of simulated ^{10}B isomerization were generated from programs written in BASIC and executed on a microcomputer. Details of the programs and program listings are in the supplementary material, while the general features are described in the Experimental Section. The number of cycles included in the comparison were adjusted to cause the B(3,6) and B(4,5,7,11) concentrations to cross at approximately the same point and were normalized to 910 h, the last experimental data point. In all of the comparisons the experimental values between 200 or 300 h and 900 h are high for B(4,5,7,11) and low for B(9,12) and B(8,10). The generality of this observation suggests a possible systematic error in phasing the NMR spectra of the three or four samples in this intermediate time region. Figure 5c shows a comparison between the thermolysis data and rearrangement via a cube-octahedral intermediate in which a single triangular face is rotated by 120° before re-forming the icosahedron. Agreement with the experimental B(3,6) and B(4,5,7,11) ^{10}B concentrations is very good for this mechanism, but significant deviation is noted from the experimental B(8,10) ^{10}B concentration.

The mechanism compared in Figure 5b involves a limited set of 12-vertex nido intermediates formed by the preferential opening of only B–B connectivities. Each intermediate undergoes a diamond–square–diamond rearrangement and then closes to an icosahedron. This mechanism gave very good agreement with the experimental thermolysis data.

A simple cuboctahedral mechanism (Figure 2a) does not allow the label to move into the B(9,12) position. We also tested the rotation of pentagonal pyramids, which showed an insignificant separation of the B(9,12) and B(8,10) values in contrast to the experimental results.

The observation that mechanisms of such great conceptual diversity showed such similar movement of an isotopic label lead us to write a program that simulated random exchange between

(25) Salinger, R. H.; Frye, C. L. *Inorg. Chem.* **1965**, *4*, 1815–1816.

adjacent boron positions in *o*-carborane. Very good agreement was observed between this random rearrangement mechanism and the experimental data. Except for the B(8,10) values, the results of random rearrangement are also very similar to those of the nido mechanism in which only B–B connectivities were initially opened (Figure 5b).

We currently favor an *o*-carborane to *o*-carborane isomerization mechanism that involves a 12-vertex nido intermediate that is arrived at by the initial opening of only B–B connectivities but note that establishment of a unique unequivocal mechanism does not appear possible on the basis of the present experimental data.

In the course of writing programs for icosahedral rearrangement mechanisms, we became aware of an equivalence between variations of the nido intermediate mechanism and several other postulated mechanisms. Figure 6 shows how these equivalencies arise. Throughout the rearrangements the atoms retain the numbers they had in the starting carborane in order to demonstrate the effect of the rearrangements on the relative atom positions. If carborane **a** opens to a 12-vertex nido intermediate, **a***, **a*** rearranges via a 2-fold diamond–square–diamond process to **b***, and **b*** then closes to form icosahedron **b**, the effect is the exchange of atoms 1 and 4. If the nido intermediate is longer lived and rearranges to **c*** before closing to icosahedron **c**, the effect, on comparison of **a** and **c**, is the rotation of a triangular face involving atoms 1,3 and 4 in carborane **a**. Further rearrangement of **c*** to **d*** and closure to icosahedron **d** produces the same result as the diamond–square–diamond twist mechanism (Figure 2d). The closure of intermediates **e*** and **f*** to **e** and **f** (not shown) does not give results similar to those of any previously postulated mechanism. This is probably because the relationship between the atoms that are rearranged in going from **a** to **e** or **f** cannot be defined by a simple geometric shape or fragment of the icosahedron. Finally, the rearrangement of the nido intermediate to **g*** brings the same atom up to the raised position that opened icosahedron **a**. A full circle of diamond–square–diamond rearrangements has rotated the entire open face relative to the rest of the cluster, and closing to icosahedron **g** gives the same result as the rotation of pentagonal pyramids in the icosahedron (Figure 2b). Figure 7 represents the six-membered open face of the 12-vertex nido intermediate schematically and illustrates the results of opening the icosahedron with atom 1 and closing after varying degrees of isomerization. The discovery that certain postulated mechanisms can be considered special cases of the nido intermediate rearrangement mechanism provides possible insight into other icosahedral carborane rearrangements. If the rearrangements are taking place via nido intermediates, then a change of substituents or a change of isomers would be expected to influence the energies and lifetimes of the various possible intermediates leading to product distributions that may be quite different even though they are formed by a fundamentally similar mechanism.

Experimental Section

Apparatus. A Lindberg 12-in. split-tube furnace was controlled with an Omega Engineering Series CN-2000 programmable temperature controller. Thin-layer rotary chromatography was performed on a Chromatotron from Harrison Research, Palo Alto, CA. Preparative thin-layer rotary chromatography plates were prepared with PF-254 silica gel with type 60 TLC $CaSO_4 \cdot {}^1/_2H_2O$ (Merck). Quartz NMR tubes (703 PQ) were purchased from Wilmad Glass Co. The ^{10}B and ^{11}B NMR spectra were obtained at 53.73 and 160.46 MHz, respectively, on a Bruker AM-500 spectrometer and were referenced to $BF_3 \cdot OEt_2$ with positive chemical shifts downfield. Infrared spectroscopy was performed on a Beckman 4220 spectrophotometer. High-resolution mass spectra were obtained by GC–MS on a Kratos MS-25 spectrometer.

Starting Materials. Diethyl ether and tetrahydrofuran were stored over and vacuum-distilled from Na/benzophenone. Dichloromethane was distilled from P_2O_5 and stored over 3-Å molecular sieves. Hexane was distilled from Na/K alloy and stored over 3-Å molecular sieves. Pentane was dried over Drierite and stored in a vacuum flask from which it was vacuum-distilled as needed. Hydrogen chloride (Matheson) was purified by repeated passage through a −126 °C U-trap into a −196 °C U-trap. $BF_3 \cdot CaF_2$ (96.24 mol % ^{10}B) was purchased from Eagle Picher Industries, Miami, OK. ^{10}B-enriched boron trifluoride was liberated from this complex with use of a procedure adapted from one obtained from the supplier: the complex was outgassed by heating at 90 °C for 5 h in

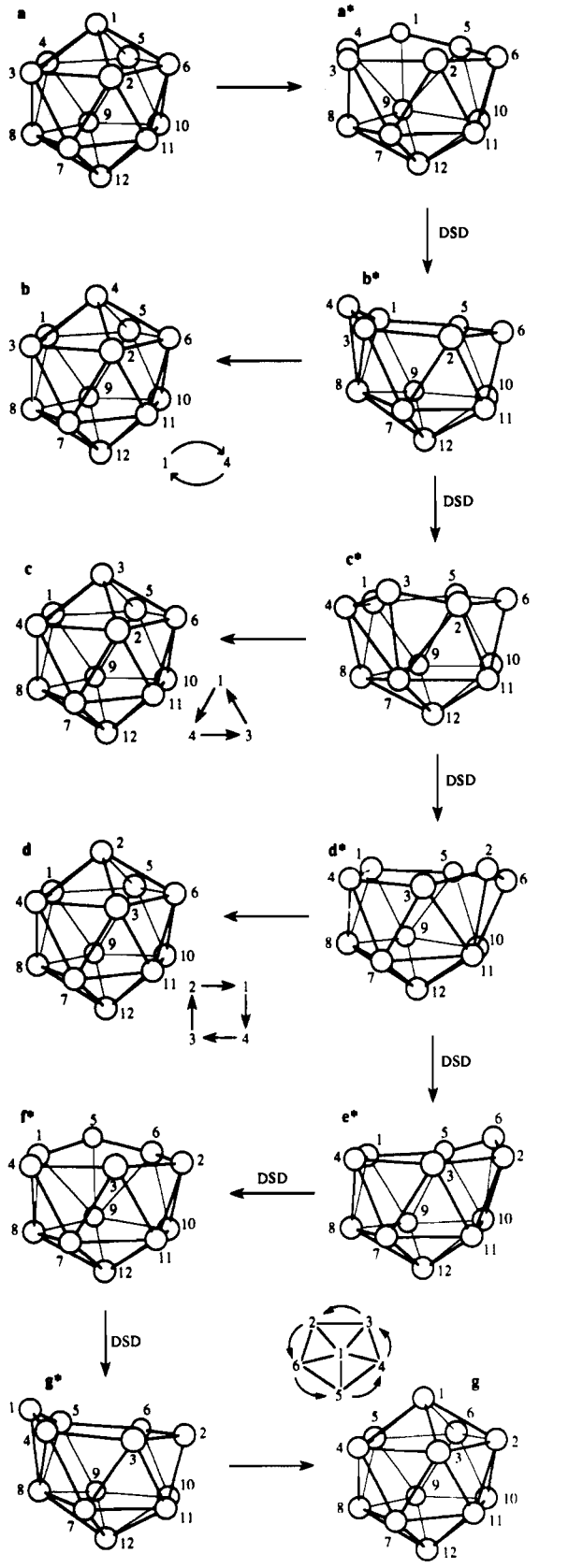

Figure 6. Rearrangements of an icosahedron, showing the equivalence of the nido intermediate mechanism and several other postulated mechanisms. Throughout the rearrangements the atoms retain the numbers they had in the starting carborane in order to illustrate the effect of the rearrangements on the relative atom positions. Specifically, **a** → **b** = exchange between adjacent borons, **a** → **c** = rotation of triangular face in the icosahedron, **a** → **d** = diamond–square–diamond twist (square face rotation), and **a** → **g** = rotation of pentagonal pyramids in the icosahedron.

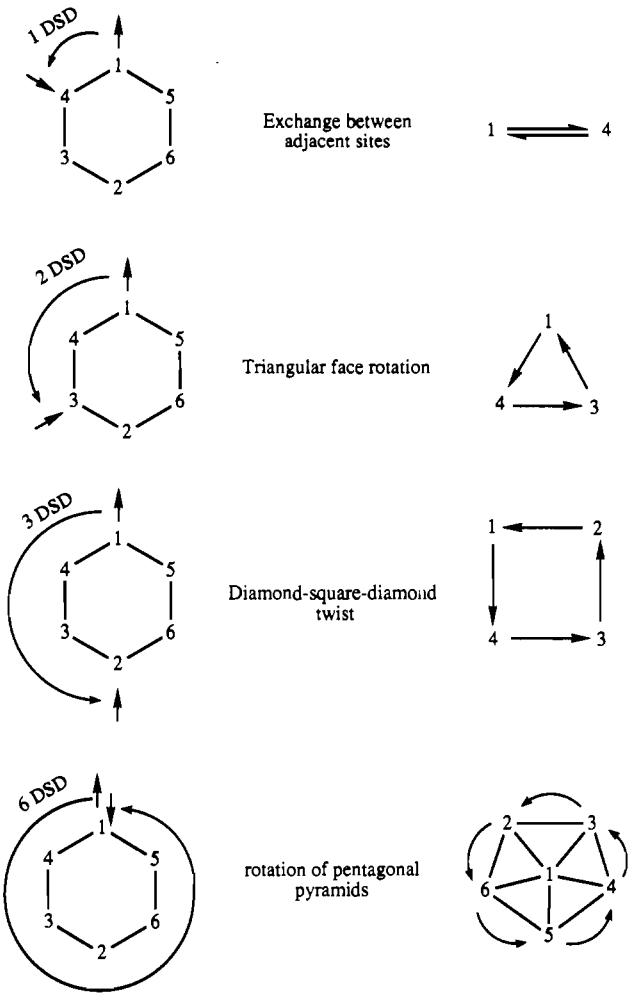

Figure 7. Schematic representation of the six-membered open face of the 12-vertex nido intermediate, showing the results of opening a pentagonal fragment of the icosahedron with atom 1 and closing with the atom that has an arrow directed at it after the indicated number of diamond–square–diamond operations.

a stainless steel tube attached to a high-vacuum line. The $^{10}BF_3$ was subsequently collected in a −196 °C U-trap as the temperature of the stainless steel tube was raised slowly from 200 to 350 °C and purified by passage through a −126 °C U-trap into a −196 °C U-trap. ^{10}B-enriched diborane(6) was obtained from $^{10}BF_3$ by modifications on a published procedure.[26] Modifications included the use of 1,2-dimethoxyethane in place of diethyl ether to complex the BF_3 and to act as solvent and the use of helium in place of nitrogen to carry the $^{10}B_2H_6$ into the vacuum line. The $^{10}B_2H_6$ was purified by repeated passage through a −126 °C U-trap into a −196 °C U-trap. The $^{10}B_2H_6$ was dissolved in tetrahydrofuran prior to the preparation of $H^{10}BCl_2$ according to the published procedure.[23] This procedure was also modified by the use of diethyl ether as solvent to make a 1.0 M solution of $H^{10}BCl_2$. The 1,2-$C_2B_{10}H_{12}$ was purchased from Dexsil Corp., Hamden, CT, and was sublimed prior to use. 1,7-$C_2B_{10}H_{12}$ was from Olin Mathieson Chemical Corp. and was sublimed prior to use. The trimethylammonium salts of *o*- and *m*-$C_2B_9H_{11}^-$ were prepared according to the published procedures.[27] The *o*- and *m*-dicarbollide ions, $C_2B_9H_{11}^{2-}$, were prepared according to the published procedures.[27,24] The 3-fluoro-3-(^{10}B)-1,2-$C_2{}^nB_9H_{11}$ was prepared according to the published procedure for 3-fluoro-1,2-$C_2B_{10}H_{11}$[24] with 96% $^{10}BF_3$ in place of BF_3.

Preparation of 3-(^{10}B)-1,2-$C_2{}^nB_9H_{12}$. The method of Hawthorne[22] for the reconstruction of the C_2B_{10} structure by boron atom insertion with $C_2B_9H_{11}^{2-}$ ions was modified by the use of $H^{10}BCl_2$ as the dichloroborane reagent for insertion. The ^{10}B-enriched *o*-carborane produced was purified by thin-layer rotary chromatography using hexane and dichloromethane as eluants and was then sublimed and dissolved in pentane, with the solution analyzed by ^{10}B and ^{11}B NMR spectroscopy.

Preparation of 2-(^{10}B)-1,7-$C_2{}^nB_9H_{12}$. The use of $H^{10}BCl_2$ as an insertion reagent with *m*-$C_2B_9H_{11}^{2-}$ was found to produce ^{10}B-enriched 1,7-$C_2B_{10}H_{12}$. The procedure used was similar to that used for the insertion reactions of *m*-$C_2B_9H_{11}^{2-}$ with trihaloboranes and aminodihaloboranes.[24] The ^{10}B-enriched *m*-carborane was purified by sublimation and analyzed by ^{10}B and ^{11}B NMR spectroscopy.

Thermal Rearrangements. Typically, a sample of about 10 mg of recently sublimed carborane was again sublimed under dynamic vacuum and condensed at −78 °C between constrictions 10–12 cm apart in a 7-mm-o.d. Pyrex tube. While under vacuum, the tube was sealed off at the constrictions. In order to minimize the large temperature fluctuations in the tube furnace, the samples were placed inside a copper block that was then heated in the furnace. The 30-mm-o.d. copper rod was 15 cm long and had four 8-mm holes around the center. These were drilled nearly the full length of the rod and could be used for heating four samples simultaneously. A central 4-mm hole for the thermocouple of the temperature controller was drilled 10 cm deep from the opposite end. A 1.5-cm piece of 30-mm-o.d. copper block was used to cover the open end of the thermolysis holes during heating. The temperature controller used was able to maintain a set temperature within ±1 °C at the controlling thermocouple. An independent thermocouple thermometer was placed inside the thermolysis tube holes and, for a set point temperature of 450 °C over a period of about 0.5 h, the temperature was found to vary by 3 °C over the length of the tubes. We conclude that a conservative error in the temperature for our thermolysis experiments is ±2 °C.

For thermolysis experiments of *m*-carborane and 2-(^{10}B)-*m*-carborane, in which we were trying to detect either *o*-carborane or ^{10}B rearrangement, the thermolysis tube was broken open and the pieces of the tube with its contents were placed immediately into a flask from which the volatile components were sublimed, as described below, for NMR analysis.

Separations. *o*- and *m*-Carborane from thermal rearrangements of 3-(^{10}B)-*o*-carborane were separated by thin-layer rotary chromatography. Thermolysis samples were broken open, and the contents were dissolved in hexane with the solutions introduced onto a 1 mm thick silica gel plate. The eluting solvents were as follows: 20 mL of hexane; 20 mL of hexane with 2.5% CH_2Cl_2 and 0.1% MeOH; 30 mL of a 7/3 mixture of hexane and CH_2Cl_2 with 0.1% MeOH; 30 mL of CH_2Cl_2 with 0.1% MeOH. Fractions of 8-mL volume were collected, with *m*-carborane generally appearing in fractions 3–5, and *o*-carborane appearing in fractions 9–11. *o*- and *m*-Carborane separated in this way were pure as determined by ^{10}B and ^{11}B NMR spectroscopy.

Separation of the rearrangement products from the thermolysis of 3-fluoro-3-(^{10}B)-*o*-carborane was accomplished by slight modifications to the *o*- and *m*-carborane separation scheme. The first of four components to elute was identified as 2-fluoro-1,7-$C_2B_{10}H_{11}$ on the basis of the symmetry in its ^{10}B and ^{11}B NMR spectra and by a comparison of its infrared spectrum with that published for 2-fluoro-*m*-carborane.[24] The last component to elute was the starting material, 3-fluoro-*o*-carborane. The remaining two components were not fully characterized.

NMR Procedures. Spectra were acquired unlocked at 300 K. The shims were tuned by observing the ^{1}H FID signal with the decoupler coils. A sweep width of 1200 and 3700 Hz was used for ^{10}B and ^{11}B, respectively; however, the filter width (FW) and delay (DE) values were intentionally changed to values appropriate for four times the sweep width in order to eliminate distortion of the base line in the spectral region caused by filter cutoff. A receiver gain of half that calculated by the automated receiver gain routine was used. Composite-pulse ^{1}H decoupling was accomplished with a decoupler power of 20 H. The number of scans collected was 8192 and 1024 for ^{10}B and ^{11}B, respectively. The number of data points was 512, and a relaxation delay of about 1.5 times the acquisition time was used. A Gaussian multiplication (LB = −3.75, GB = 0.25) was performed on the FID followed by zero-filling twice and Fourier transformation. The spectra were phased to take into account a slight base-line roll in the vicinity of the 3,6- and 4,5,7,11-resonances of *o*-carborane and the 2,3- and 4,6,8,11-resonances of *m*-carborane. Base-line correction was accomplished by using a spline curve between base-line points chosen by inspection with the BASLPNTS routine of Bruker's DISNMR software package. Spectra acquired and processed in the above manner generally had signal to noise ratios of greater than 1000. Integrations were found to be very sensitive to the phasing constants chosen; however, a reproducibility of ±3% was obtained. The ^{10}B NMR spectrum obtained for the thermolysis sample of 2-(^{10}B)-*m*-carborane was of sufficient quality that we would have been able to detect 1 part in 5000 of *o*-carborane.

Predictions of Mechanistic Models. Programs to simulate isomerization within *o*-carborane based on several postulated mechanisms were written with the binary version of Microsoft BASIC operating on an Apple Macintosh Plus microcomputer. Specific constrants and as-

(26) Shapiro, I.; Weiss, H. G.; Schmich, M.; Skolnik, S.; Smith, G. B. L. *J. Am. Chem. Soc.* **1952**, *74*, 901–905.
(27) Hawthorne, M. F.; Young, D. C.; Garrett, P. M.; Owen, D. A.; Schwerin, S. G.; Tebbe, F. N.; Wegner, P. A. *J. Am. Chem. Soc.* **1968**, *90*, 862–868.

sumptions of these programs are outlined in the supplementary material. Within the constraints of the particular mechanism, all of the independent events that gave rise to *o*- to *o*-carborane isomerization were defined. For statistical reasons, symmetry-equivalent processes were considered as independent isomerization events. We then described the effect of each isomerization event on the relative positions of the boron atoms in *o*-carborane. A 2-dimensional array of size $n \times 10$ stored the ^{10}B concentrations for each of the 10 boron atoms for each of n independent isomerization events. The starting concentrations were those of the enriched compound: 96.2% for B(3), 20.2% for B(4)-B(12). For each isomerization event the movement of boron atoms within *o*-carborane was recorded by exchanging the appropriate concentrations in that row of the array, even if the concentrations were the same. After each independent isomerization event had occurred once, the ^{10}B concentration for each boron was averaged, and this average was used as the starting value for that boron in each event during the second cycle.

Following each cycle, the average ^{10}B concentration for each boron atom was printed out and the concentrations for the equivalent borons were added to give the intensity of a simulated resonance at that point in the isomerization. These were then compared to the normalized integrals of thermally isomerized 3-(^{10}B)-*o*-carborane as described under Results and Discussion. All of the mechanisms reached equilibrium after repeated cycles, giving rise to *o*-carborane resonances in the ratio 2:2:4:2 for B(9,12), B(8,10), B(4,5,7,11), and B(3,6), respectively. This feature served as a check on the proper functioning of the program's calculations.

Acknowledgment. We thank Dr. Bruce Adams for advice and help in the NMR experiments and the National Science Foundation for partial support of this research and for major departmental instrumentation grants.

Supplementary Material Available: A summary of rearrangement assumptions used for programming, contents of programs used for simulations, and a sample program output for the cuboctahedral intermediate with triangular face rotation (26 pages). Ordering information is given on any current masthead page.

Contribution from the Department of Chemistry,
Case Western Reserve University, Cleveland, Ohio 44106

A New Route to Alkoxysilanes and Alkoxysiloxanes of Use for the Preparation of Ceramics by the Sol–Gel Technique

George B. Goodwin and Malcolm E. Kenney*

Received September 7, 1988

The preparation of $(EtO)_4Si$ from $Ca_3(SiO_4)O$, Ca_2SiO_4, and portland cement, $(EtO)_3SiOSi(OEt)_3$ from $Ca_2Zn(SiO_3)_2O$, $(n\text{-}PrO)_3SiOSi(O\text{-}n\text{-}Pr)_2OSi(O\text{-}n\text{-}Pr)_3$ from $Ca_3(SiO_3)_3$, $[(EtO)_2SiO]_4$ from $Ca_8(SiO_3)_4Cl_8$, and the bicyclic [5.5.1]- and [5.3.3]-isomers of $(EtO)_{10}Si_6O_7$ from $Cu_6(SiO_3)_6 \cdot 6H_2O$ and $Na_4Ca_4(SiO_3)_6$ is described. The route employed in these preparations has two variations. Both can be described in terms of three steps. In one, the synthesized silicate variation, the first step is the conversion of silica or an available silicate to a silicate having an ion with a framework that is the same as that of the product or similar to it. The second is either the conversion of this silicate to a silicic acid that is solvated by an alcohol and has a framework that is the same as or similar to that of the product or the conversion of this silicate to one or more corresponding partially alkoxylated silicic acids. The third is the conversion of the silicic acid or acids to the product. In the second, or the available silicate variation, the first step entails the acquisition of a silicate with the needed framework from natural or other sources and the last two steps involve conversions that are the same as those in the synthesized silicate variation. The procedures and conditions used in the route are discussed.

In the past few years tetraalkoxysilanes have been used frequently for the preparation of ceramics by the sol–gel process.[1-3] Very recently oligomeric alkoxysiloxanes have been considered for this same purpose.[4] Accordingly, good routes to these two types of compounds are of interest.

Here we present a simple new route to them. The route entails the conversion of a silicate to a silicic acid and then to the desired alkoxysilane or alkoxysiloxane.[5]

Two precedents for the route are provided by the conversion of sodium silicate solutions to polymeric alkoxysiloxanes[11] and the conversion with apparent framework retention of chrysotile asbestos, $Mg_3Si_2O_5(OH)_4$, to a polymeric allyloxysiloxane.[12] Another precedent is provided by the conversion to a very small extent (as a result of a byproduct reaction) of pseudowollastonite, $Ca_3(SiO_3)_3$, to $[(i\text{-}PrO)_2SiO]_3$.[13] A more distant precedent is furnished by the conversion of various metal silicates to oligomeric organosiloxysiloxanes.[14]

Experimental Section

$(EtO)_4Si$ from Tricalcium Silicate, $Ca_3(SiO_4)O$. An HCl–ethanol solution (7.54 N, 54.9 mL) was added slowly (9 mL/min) to a stirred, cooled (−10 °C) suspension of monoclinic tricalcium silicate, $Ca_3(SiO_4)O$, (Construction Technology Laboratories, Inc., Skokie, IL; powdered, 15.0 g) in ethanol (500 mL). The resulting mixture was added (~22 mL/min) to a solution of ethanol (500 mL) and toluene (1100 mL) that was being distilled (1 atm) at a moderate rate (~17 mL/min). After the addition had been completed, the distillation was continued until the amount of distillate was substantial (1.83 L). The remainder was filtered, and the solid was washed with pentane (75 mL). The filtrate and washings were combined, and the resulting solution was distilled. An

(1) *Ultrastructure Processing of Ceramics, Glasses and Composites*; Hench, L. L., Ulrich, D. R., Eds.; John Wiley: New York, 1984.
(2) *Better Ceramics Through Chemistry*; Brinker, C. J., Clark, D. E., Ulrich, D. R., Eds.; North Holland: New York, 1984.
(3) *Better Ceramics Through Chemistry II*; Brinker, C. J., Clark, D. E., Ulrich, D. R., Eds.; Materials Research Society: Pittsburgh, PA, 1986.
(4) Day, V. W.; Klemperer, W. G.; Mainz, V. W.; Millar, D. M. *J. Am. Chem. Soc.* **1985**, *107*, 8262.
(5) Preliminary accounts describing this route have been published,[6-8] and patents pertaining to it have been issued.[9,10]
(6) Goodwin, G. B.; Kenney, M. E. *Polym. Prepr. (Am. Chem. Soc., Div. Polym. Chem.)* **1986**, *27*, 107.
(7) Goodwin, G. B.; Kenney, M. E. In *Inorganic and Organometallic Polymers*; Zeldin, M., Wynne, K. J., Allcock, H. R., Eds.; ACS Symposium Series 360; American Chemical Society: Washington, DC, 1988; p 238.
(8) Goodwin, G. B.; Kenney, M. E. In *Silicon-Based Polymer Science: A Comprehensive Resource*; Ziegler, J. M., Fearon, F. W. G., Eds.; Advances in Chemistry Series 224; American Chemical Society: Washington, DC, 1990; p 251.
(9) Kenney, M. E.; Goodwin, G. B. U.S. Patent 4717773, 1988.
(10) Goodwin, G. B.; Kenney, M. E. U.S. Patent 4824985, 1989.
(11) Kirk, J. S. U.S. Patent 2395880, 1946.
(12) Bleiman, C.; Mercier, J. P. *Inorg. Chem.* **1975**, *14*, 2853.
(13) Calhoun, H. P.; Masson, C. R. *J. Chem. Soc., Dalton Trans.* **1980**, 1282.
(14) Lentz, C. W. *Inorg. Chem.* **1964**, *3*, 574.

0020-1669/90/1329-1216$02.50/0